FUDMA Journal of Sciences (FJS)
ISSN online: 2616-1370
ISSN print: 2645 - 2944
Vol. 10 No. 12, June, 2026, pp 168 – 186
DOI: https://doi.org/10.33003/fjs-2026-1012-5090

Hydrothermal Mineralization Potential Mapping Using AHP Integration of Airborne Geophysical Data over the Southern Benue Trough, Nigeria

***[1]Stella C. Okenu, [2,3]Olatunji S. Ayaninnuola and [3]Abu Mallam**

[1]Physics Department, Nasarawa State University, Keffi, Nasarawa State, Nigeria.
[1]Physics Advanced Research Centre, Sheda Science and Technology Complex (SHESTCO), FCT Abuja, Nigeria.
[2]Physics Department, University of Abuja, FCT Abuja, Nigeria.

*Corresponding authors' email: stellaokenu720@gmail.com

ABSTRACT

Mineral exploration has gradually shifted from traditional field mapping to integrated geophysical techniques capable of investigating large areas quickly and economically. Hydrothermal mineral deposits are controlled by several geological factors, including faults, fractures, intrusive bodies, hydrothermal alteration, and lithological variations. The Analytical Hierarchy Process (AHP) was employed to delineate the hydrothermal mineralization potential of the Southern Benue Trough, Nigeria, using integrated high-resolution aeromagnetic and airborne radiometric datasets. Advanced geophysical enhancement techniques, like Reduction to the Equator (RTE), First Vertical Derivative (FVD), Analytical Signal (AS), Source Parameter Imaging (SPI), Spectral Analysis, and Centre for Exploration Targeting (CET) grid analysis, were applied to investigate subsurface structures, lithological contacts, intrusive bodies, and basement configurations and depth to magnetic sources. The Analytical Signal map classified the study area into high (>0.0166nT/m), intermediate (0.0093–0.0166 nT/m), and low (<0.0093 nT/m) magnetic zones. High magnetic zones were interpreted as intrusive and structurally disturbed regions associated with hydrothermal activity. SPI depth estimates revealed shallow magnetic source bodies ranging from <0.10 km to >2.7 km, while spectral analysis revealed deeper magnetic source depths ranging from 2.08 km to 9.02 km, with an average depth of 5.01 km. The resulting basement depth model revealed an undulating basement morphology characterized by horsts and grabens that served as depocenters for thick sedimentary accumulations. Structural analysis from the CET grid revealed dominant NE–SW trends with subordinate E–W, WNW–ESE, and NW–SE orientations, reflecting the influence of Pre-Pan-African and Pan-African tectonic events. Areas of high lineament density correspond closely with zones of high magnetic amplitudes, indicating structurally controlled hydrothermal fluid migration. Radiometric datasets comprising equivalent uranium (eU), equivalent thorium (eTh), potassium (K %), ternary maps, and K/eTh ratio maps were used for lithological discrimination and hydrothermal alteration mapping. The AHP-integrated prospectivity model delineated high, moderate, and low hydrothermal mineralization potential zones across the Southern Benue Trough.

Received: 18th May 2026
Accepted: 15th July 2026
Published: 30th July 2026

Keywords: Hydrothermal mineralization, Southern Benue Trough, Aeromagnetic data, airborne radiometric data, Analytical Hierarchy Process (AHP)

INTRODUCTION

The availability of raw materials, particularly Lead, zinc and Barite mineral, was a fundamental driver of the Industrial Revolution in the late eighteenth century, forming the backbone of industrial machinery, transportation systems, and engineering infrastructure. Most modern industrial products like automobiles, railways, and heavy equipment originate from mineral resources extracted from the Earth's subsurface. Despite significant technological advancements, nations across the world continue to depend heavily on these resources to sustain industrial growth, develop infrastructure, and improve living standards. Consequently, global demand for minerals has intensified, as countries strive to secure the material required for sustainable economic development and industrial competitiveness (International Energy Agency, 2025; World Nuclear Association, 2024; British Geological Survey, 2022). Nigeria, the most populous country in Africa, relies predominantly on hydropower and fossil fuels for electricity generation, with increasing contributions from renewable sources such as solar and wind energy. However, nuclear and geothermal energy is currently contributing about 10% of global electricity generation and offering a low-carbon alternative, has not yet been fully developed in the country (International Atomic Energy Agency, 2024). In contrast, countries such as France, Ukraine, and Finland have successfully integrated nuclear energy into their electricity mix, reflecting a strategic utilisation of mineral and energy resources for sustainable power generation. Nigeria possesses significant potential to adopt a similar approach however, achieving this requires extensive geological and geophysical exploration to identify economically viable solid minerals and assess the radioactive potential of subsurface formations.

In mineral exploration, the integration of geophysical methods in particular magnetic and radiometric techniques has become a powerful and widely adopted approach. Rather than relying solely on the direct detection of ore bodies, these methods focus on identifying indirect indicators such as hydrothermal alteration zones and structurally controlled features that favour mineralisation. The integration of magnetic and radiometric datasets has been shown to enhancesubsurface resolution and improve the delineation of exploration targets (Ogunsanwo et al., 2025; Abdelrady et al., 2024). Magnetic surveying plays a critical role in detecting variations in the Earth's magnetic field caused by contrasts in magnetic susceptibility within subsurface geological formations. These variations generate anomalies commonly associated with mineral systems such as sulphide deposits and iron-rich bodies. Advanced processing techniques, First Verical Derivatives (FVD), Analytic Signal (AS), Spectral Analysis (AS) and Source Parameter Imaging (SPI) was used for mapping of faults, fractures, depths to magnetic sources and intrusive bodies that act as conduits for mineralising fluids (Akingboye et al., 2025). On the other hand, radiometric methods was analysed based on the distribution of potassium (K), thorium (Th), and uranium (U), provided valuable insights into lithological variations and hydrothermal alteration processes. Radiometric ratios such as K/Th and U/Th are widely used to delineate alteration zones associated with mineralisation (Ohaegbuchu et al., 2026).

Within the Southern Benue Trough, mineralization is dominated by lead–zinc sulphides, barite, saline/brine occurrences, and minor phosphate deposits hosted mainly within Cretaceous sedimentary sequences. These mineral deposits are strongly controlled by regional fault systems, fractures, and basin-scale tectonic structures that acted as conduits for hydrothermal fluids during mineral deposition (Olade, 1976; Farrington, 1952; Akande & Mücke, 1993; Obiora et al., 2015). Consequently, integrated geophysical investigations have become increasingly important for delineating favourable mineralized zones in the basin. High-resolution aeromagnetic data have been widely applied to map basement structures, fault systems, intrusive bodies, and lithological contacts that influence mineralization, whereas airborne radiometric data provide complementary information on lithological variations and hydrothermal alteration through the spatial distribution of potassium (K), thorium (Th), and uranium (U) radioelements (Dentith & Mudge, 2014; Abdelrady et al., 2023, 2024). The integration of these complementary datasets enhances geological interpretation by establishing spatial relationships between structural features, alteration zones, and potential mineralized targets.

In structurally complex terrains such as the Southern Benue Trough, mineral prospectivity mapping is fundamentally a spatial decision-making problem that requires the integration of multiple geological and geophysical variables. Numerous studies have demonstrated that integrated geophysical analysis significantly reduces exploration uncertainty and improvesexploration efficiency by identifying structurally controlled mineralization pathways and hydrothermal alteration signatures that may not be recognized using individual datasets (Carranza, 2009; Carranza, 2011; Abdelrady et al., 2023; Eldosouky et al., 2024). The integration of aeromagnetic and radiometric datasets is therefore widely regarded as an effective approach for regional mineral exploration because it simultaneously captures both structural controls and lithological variations associated with hydrothermal systems.

To further improve mineral prospectivity modelling, multicriteria decision-making techniques such as the Analytical Hierarchy Process (AHP) have been increasingly adopted in mineral exploration. AHP provides a systematic and transparent framework for assigning relative importance to exploration criteria through pairwise comparison, thereby minimizing subjectivity and improving the consistency of mineral potential assessments (Saaty, 1980; Carranza, 2009; Yousefi & Carranza, 2015; Arabameri et al., 2021). By integrating weighted aeromagnetic and aeroradiometric parameters within a Geographic Information System (GIS) environment, AHP enables the generation of mineral potential maps that effectively highlight areas with high exploration significance. Accordingly, this study integrates airborne magnetic and radiometric datasets using an AHP-based multicriteria framework to evaluate hydrothermal mineralization potential across the Southern Benue Trough. The integrated approach seeks to reduce the uncertainty associated with single-dataset interpretation while improving understanding of the structural and hydrothermal controls on Pb–Zn and barite mineralization. The resulting prospectivity map provides a scientific basis for prioritizing exploration targets, supporting sustainable mineral resource development, and encouraging further investment in Nigeria's solid mineral sector.

Geological Setting of the Area

The Southern Benue Trough forms part of the extensive Benue Trough of Nigeria, a major NE–SW trending intracontinental rift basin that developed during the Early Cretaceous as a consequence of the separation of the African and South American plates and the opening of the South Atlantic Ocean (Benkhelil, 1989; Burke et al., 1971). The trough extends from the Niger Delta in the southwest to the Chad Basin in the northeast and is commonly subdivided into the Northern, Central, and Southern Benue Trough based on structural and stratigraphic characteristics (Obaje, 2009; Nwajide, 2013). The Southern Benue Trough as shown in (Figure 1) is characterizedby thick sedimentary successions deposited from the Albian to Maastrichtian periods and consists predominantly of marine and paralic sediments intercalated with minor volcanic and intrusive rocks (Benkhelil, 1989; Obaje, 2009). The basin evolution involved episodes of crustal extension, subsidence, sedimentation, magmatism, and tectonic inversion associated with Santonian compressional deformation. Structurally, the region is marked by extensive faulting, folding, fracturing, and tectonic reactivation, which significantly influenced sedimentation patterns, magmatic emplacement, and hydrothermal mineralization within the basin (Nwajide, 2013). The study area is underlain predominantly by sedimentary sequences of the Southern Benue Trough and crystalline basement rocks of the adjoining Oban Massif. The Oban Massif forms part of the Precambrian Basement Complex of southeastern Nigeria and consists mainly of migmatites, granite gneisses, schists, amphibolites, and granitoids reworked during the Pan-African orogeny (~600 Ma) (Rahaman, 1988). These basement rocks constitute the structural foundation upon which the Benue Trough sedimentary sequences were deposited.

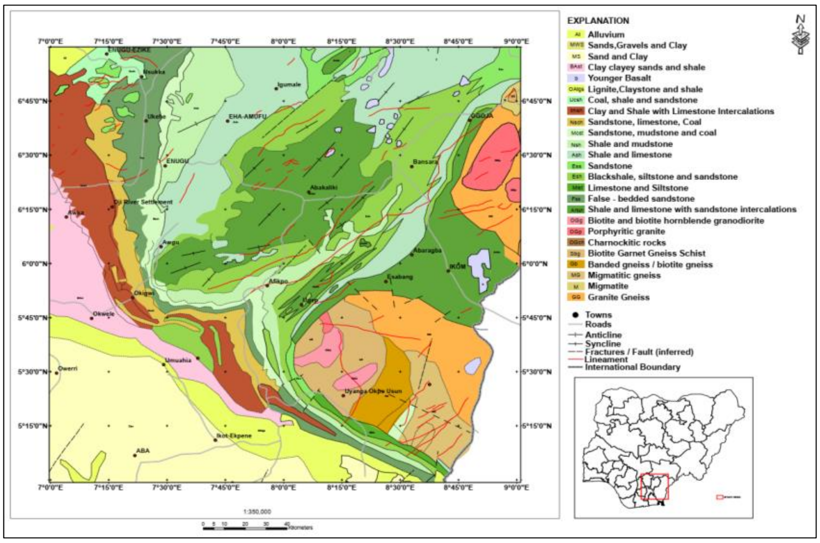

Figure 1: Geological Map of the study area (Modified after NGSA, 2022)

The principal lithostratigraphic units within the Southern Benue Trough include the Asu River Group, Eze-Aku Formation, Awgu Formation, and Nkporo Group (Figure. 2). The Asu River Group, which forms the oldest sedimentary unit of Albian age, consists predominantly of dark gray to black shale, siltstone, limestone, sandstone, and minor volcanic rocks deposited under marine conditions (Reyment, 1965; Nwajide, 2013). This formation is extensively fractured and intruded by numerous igneous bodies, particularly along major tectonic zones. The Asu River Group hosts significant lead–zinc and barite mineralization associated with hydrothermal activity and structurally controlled fluid migration (Akande & Abimbola, 1987). Overlying the Asu River Group is the Cenomanian–Turonian Eze-Aku Formation, composed mainly of calcareous shale, sandstone, limestone, and siltstone deposited in shallow marine environments (Obaje, 2009). The Eze-Aku Formation is followed by the Coniacian Awgu Formation, which consists predominantly of shale, sandstone, and limestone units reflecting alternating marine and marginal marine depositional environments (Nwajide, 2013). The Maastrichtian Nkporo Group forms the uppermost stratigraphic sequence and comprises dark shale, mudstone, sandstone, and coal-bearing horizons deposited during a major marine transgressive phase (Reyment, 1965).

Structurally, the Southern Benue Trough exhibits dominant NE–SW structural trends with subordinate NW–SE and E–W orientations, reflecting multiple phases of tectonic deformation associated with the Pan-African orogeny and subsequent Santonian tectonism (Benkhelil, 1989; Anudu et al., 2014). The Santonian tectonic event caused intense folding, uplift, faulting, and basin inversion, leading to the development of numerous fractures and fault systems that presently serve as conduits for hydrothermal fluid circulation and mineralization. The region also contains localized igneous intrusions and volcanic bodies emplaced during tectono-magmatic episodes. These intrusions contribute significantly to the magnetic signatures observed across the basin and are believed to play an important role in controlling hydrothermal mineralization processes (Oha et al., 2016). Geophysical studies indicate that the interaction between basement structures, intrusive activity, and sedimentary architecture strongly controls the tectono evolution of the Southern Benue Trough.

Hydrothermal mineralization within the basin is largely structurally controlled and commonly associated with faults, fractures, and intrusive contacts. Economically important mineral deposits within the Southern Benue Trough include lead–zinc, barite, fluorite, and associated sulfide mineralization, particularly within the Abakaliki and Ishiagu areas (Akande & Abimbola, 1987; Farrington, 1952). These mineral occurrences are closely linked to hydrothermal fluid circulation associated with tectonic reactivation and magmatic emplacement.

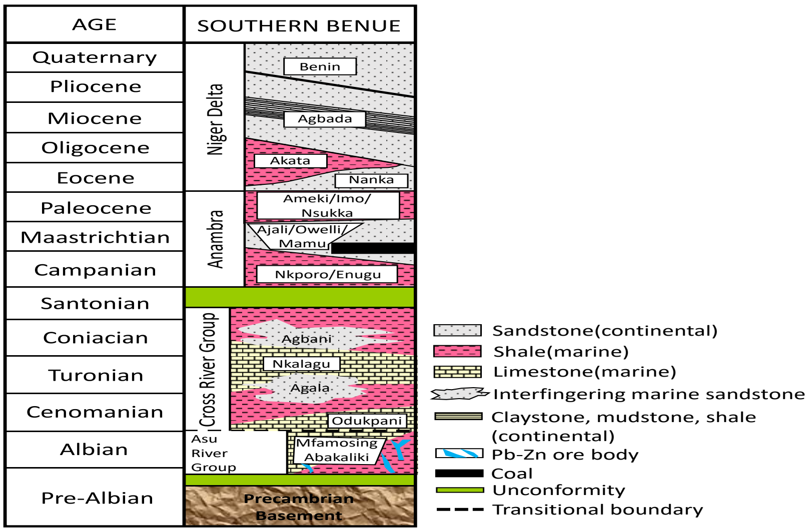

Figure 2: Stratigraphic Successions of the SBT (modified after Abubakar, 2014; Bute et al., 2024)

MATERIALS AND METHODS

The high-resolution aero-radiometric and aero-magnetic data of Nigerian sheets dataset consists of sixteen (16) sheets (287, 288, 289, 290, 301, 302, 303, 304, 312, 313, 314, 315, 321, 322, 323, and 324), while the airborne radiometric dataset covers thirteen (13) sheets within the study area (Figure. 1). (on the scale of 1:100, 000) was obtained from the Nigeria Geological Survey Agency, Abuja, Nigeria (NGSA). Table 1 contains the essential acquisition parameters. However, otherdetails can be found on the NGSA website (ngsa.gov.ng). Both data were analysed using Geosoft (Oasis Montaj) version 8.5, ArcGis 10.5, and excel software

Table 1: Acquisition Parameters Used for Airborne Magnetic and Radiometric Survey in the Research Area

Parameter	Survey specification
Mean sensor ground clearance	**80m**
Flight line separation	0.5 km
Interval of tie line	5 km
Recording interval	0.1 s

Aeromagnetic Data

The data gotten from NGSA was in the form of a total magnetic intensity (TMI) grid merged together to a total study area coverage. The magnetic inclination (− 0.36) and declination (− 1.83) were obtained based on the International Geomagnetic Reference Field (IGRF) 2005. Magnetic data processing involves systematic correction, transformation, enhancement, and interpretation of total magnetic intensity (TMI) data to isolate anomalies caused by subsurface geological bodies. Standard processing steps include diurnal correction, IGRF removal, filtering, reduction to equator (RTE), derivative enhancement, analytic signal computation, and structural analysis using CET tools.

The RTE filter is usually performed on aeromagnetic data obtained in low magnetic latitude regions (< 15°) like Nigeria, to ensure that the anomaly peaks are centered symmetrically on top the causative bodies responsible for them (Vacquier *et al.*, 1951). Magnetic survey information from areas where Earth's geomagnetic field inclination is within the range of ±20 is usually subjected to RTE processing to ascertain that the anomalies align perfectly on the magnetic ensembles where it is emanating from (Leu, 1981; Gibert and Galdeano, 1985). The equation found in (Leu, 1981) can be used to generate the RTE result. The RTE grid was further subjected to several filtering techniques to enhance qualitative and quantitative interpretation signal. Table 2 has a summary of the filtering techniques employed in this study.

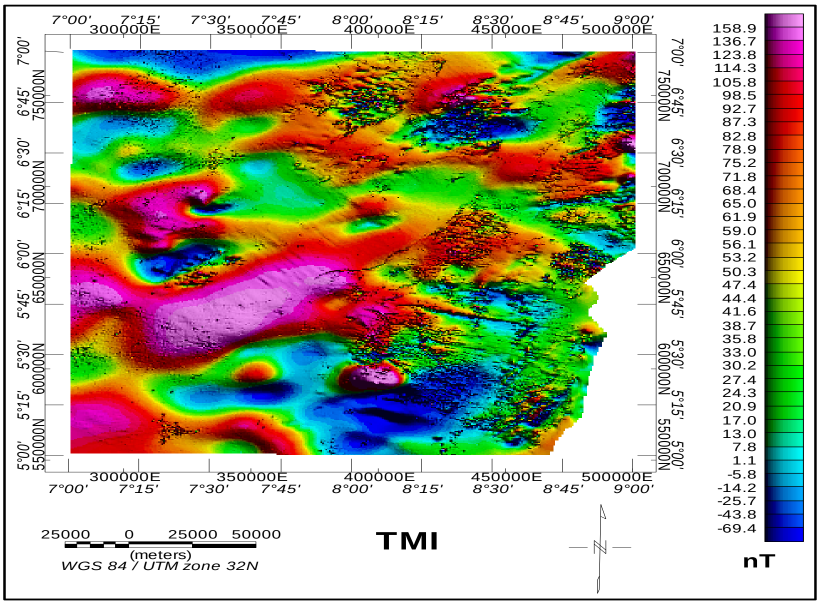

Figure. 3: Total Magnetic Intensity map of the study area

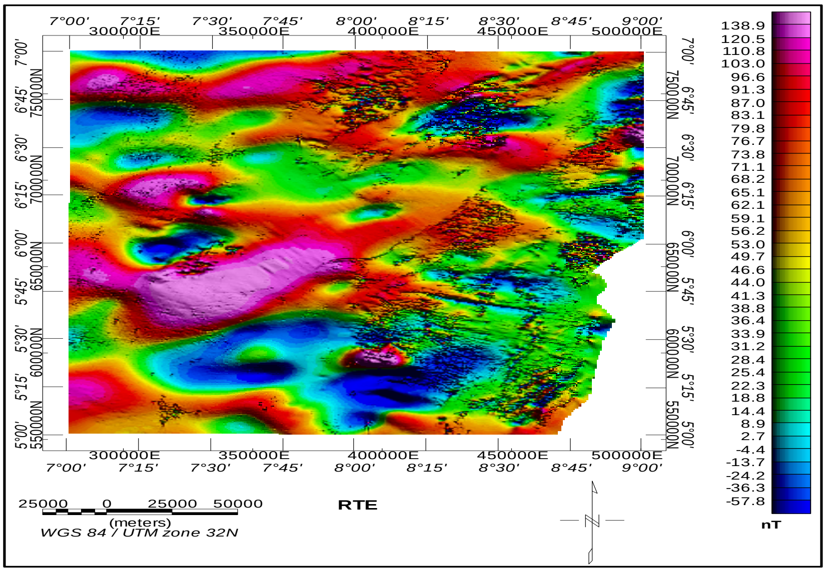

Figure 4: RTE map of the study area

Table 2: Signal Enhancement Technique Used for the Aero-Magnetic Data

Filtering Techniques	Definition	Application
Reduction to the Equator	It is an algorithm that accounts for a spatial shift, especially in an equatorial Zone. (Leu, L.-K., 1982; Li, Y. & Oldenburg, D. W. Stable, 2001)	It is used to place the magnetisation of a geologic body over its causative. Sources. (Maurice, Z. E. O, 2023; Gabtni, H. & Jallouli, C, 2017)
Regional-residual separation	It is the most efficient procedure to obtain residual field (Gabtni, H. & Jallouli, C, 2017). The residual field is the deviation from the regional field and is considered the target source susceptibility(Agocs, W. B 191)	To reveal good target source susceptibility for exploration (Allek, K., Boubaya et al., 2016; Akanbi, E. S. & Mangset, W. E, 2011)
Vertical gradient	It is defined as the gradient of magnetic intensity (Dentith, M. & Mudge, S. T, 2014) given as: $\frac{\partial MI}{\partial z}$ (1) where MI is the magnetic intensity	To enhance and highlight shallow features and sharpen the edges of anomalous bodies(Núñez-Demarco et al, 2023)
Analytic Signal (AS)	According to (Nabighian, M. N, 1972) AS is given as: $\sqrt{\left(\frac{\partial MI}{\partial x}\right)^2 + \left(\frac{\partial MI}{\partial y}\right)^2 + \left(\frac{\partial MI}{\partial z}\right)^2}$ (2) Where $\frac{\partial MI}{\partial x}$, $\frac{\partial MI}{\partial y}$, and $\frac{\partial MI}{\partial z}$ are gradients in the x, y, and z directions, respectively	To define geologic borders and resolve and highlight anomalous sources that are closely spaced (especially in equatorial regions) (Eldosouky, A. M. *et al., 2022)*

Filtering Techniques	Definition	Application
CET grid analysis	It is a tool developed by geophysical explorers for magnetic structural Analysis (Holden, E. J, 2008; Kovesi, P, 1999; Holden, E.-J. *et al., 2010)*	To reveal magnetic lineaments (Abdelrady, M. *et al.*, 2023). This was further used to generate the lineament density map in this study
CET porphyry analysis	Like the CET grid analysis, this has to do with porphyry detection (Holden, E.-J. *et al., 2010)*	To reveal intrusive porphyry centres (Osinowo, O. O. et al., 2020)

Aero-radiometric Data

Radiometric surveys measure naturally occurring gamma radiation emitted from radioactive isotopes present within the Earth's crust. The principal contributors to terrestrial gamma radiation are potassium (K), uranium (U), and thorium (Th), which are the dominant naturally occurring radioelements detected in airborne gamma-ray spectrometry surveys (IAEA, 2021; Minty, 2023). These radioelements emit characteristic gamma-ray energies that allow their concentrations to be estimated and spatially mapped.

Unlike many geophysical methods that investigate contrasts in physical properties at significant depths, radiometric surveys are primarily sensitive to the uppermost portion of the Earth's surface, typically penetrating only a few tens of centimeters into the ground depending on soil moisture, vegetation cover, and surface composition (Dentith & Mudge, 2014; IAEA, 2021). Consequently, airborne radiometric data are particularly valuable for mapping surface and near-surface geochemical variations rather than deeper physical structures. Because the emitted gamma-ray energies are element-specific, radiometric methods occupy an important interface between geophysics and geochemistry.

High-resolution airborne radiometric surveys are widely applied in lithological mapping, structural interpretation, hydrothermal alteration detection, environmental studies, and mineral exploration due to the distinct radioactive signatures of different rock types and alteration zones (Dentith & Mudge, 2014; Elkhateeb & Abdellatif, 2018; Minty, 2023). Variations in potassium, uranium, and thorium concentrations provide important information on rock composition, alteration processes, and the distribution of radioactive minerals. Hydrothermal processes often redistribute potassium and uranium, whereas thorium generally remains relatively immobile, making radioelement ratios particularly useful for identifying alteration zones associated with mineralization.

The integration of potassium (K), equivalent uranium (eU), equivalent thorium (eTh), and ternary radiometric images enhances lithological discrimination and mineral prospectivity interpretation. In particular, radioelement abundance ratios such as eU/eTh, eU/K, and K/eTh are commonly more diagnostic of lithological variation and hydrothermal alteration than individual radioelement concentrations alone (Uyanık, 2022; Elkhateeb & Abdellatif, 2018). Elevated K/eTh ratios are widely recognized as indicators of potassic hydrothermal alteration because potassium is typically enriched during hydrothermal fluid circulation, whereas thorium remains relatively stable (Hoover et al., 1992; Elkhateeb & Abdellatif, 2018).

Spatial Integration and Correlation

Analytical Hierarchy Process (AHP)

The Analytical Hierarchy Process (AHP) was employed in this study to integrate multiple geophysical parameters for the delineation of zones favorable for hydrothermal mineralization within the Southern Benue Trough. AHP is a widely used Multi-Criteria Decision-Making (MCDM) technique that enables the systematic evaluation and weighting of different controlling factors based on their relative importance in mineral prospectivity analysis (Saaty, 1980; Saaty, 2008).

In this study, thematic layers derived from aeromagnetic and airborne radiometric data including lineament density, Analytical Signal and K/eTh ratio were integrated using the AHP framework. These parameters were selected because they represent the principal structural, thermal, and hydrothermal factors controlling fluid migration and mineral deposition within the Southern Benue Trough. Structural features such as faults and fractures provide pathways for hydrothermal fluids, while thermal anomalies and radiometric enrichment are commonly associated with hydrothermal alteration and mineralization processes (Benkhelil, 1989; Obaje, 2009). The AHP technique is based on pairwise comparison of selected criteria using a standardized preference scale ranging from 1 to 9, where 1 represents equal importance and 9 indicates extreme importance of one criterion over another as shown in Table 3.

Table 3: Basic AHP scoring scale

Score	Significance
1	Two equally important variable
3	A little more significant
5	Much more significant
7	Strongly more significant
9	Extremely more significant
2,4,6,8	Midway values between the two neighbouring judgments
½, 1/3, …1/9	These are the significance levels' reciprocals

Expert geological and geophysical judgments were used to assign relative importance values to the selected parameters according to their influence on hydrothermal mineralization. The resulting pairwise comparison matrix was subsequently normalized to derive the weight of each thematic layer (Saaty, 1980; Feizizadeh & Blaschke, 2013).

To ensure the reliability and consistency of the pairwise comparisons, a consistency check was performed using the Consistency Index (CI) and Consistency Ratio (CR). The Consistency Index was computed using:

$$CI = \frac{\lambda_{\max} - n}{n - 1} \quad (1)$$

Where λmaxis the maximum eigenvalue of the pairwise comparison matrix and n represents the number of criteria. The Consistency Ratio (CR) was then calculated as:

$$CR = \frac{CI}{RI} \quad (2)$$

Where RI is the Random Index corresponding to the number of evaluated criteria. According to (Dentith, M. C., 1994), a matrix is considered acceptably consistent when the CR value is less than 0.10. In this study, the computed CR satisfied this condition, indicating that the assigned weights and judgments are reliable for mineral prospectivity modeling. The weighted thematic layers were subsequently integrated using a GIS-based weighted overlay approach to generate a mineral prospectivity map highlighting zones favorable for hydrothermal mineralization within the Southern Benue Trough.

Factors Considered and Reclassification in the AHP Analysis

Lineament density, Analytical Signal (AS), and K/eTh ratio were considered in the hydrothermal mineralization potential assessment of the Southern Benue Trough. These parameters were selected because they represent the principal structural, magnetic, and hydrothermal indicators controlling mineral deposition within the basin. Lineament density reflects the spatial distributionand concentration of geological structures such as faults, fractures, and shear zones and dykes. These structures commonly serve as conduits for hydrothermal fluid migration and mineral deposition. Previous studies within the Benue Trough and similar tectonic environments have shown that hydrothermal mineralization is strongly controlled by structural features and zones of tectonic reactivation (Benkhelil, 1989; Anudu et al., 2014; Oha & Ekwueme, 2015). Consequently, areas characterized by high lineament density were considered highly favorable for mineralization.

The Analytical Signal (AS) was used to enhance and delineate magnetic anomalies associated with lithological contacts, intrusive bodies, and structurally controlled magnetic sources. The AS filter is particularly effective in low magnetic latitude regions such as Nigeria because it is independent of magnetization direction and clearly defines the edges of magnetic bodies (Roest et al., 1992; Nabighian et al., 2005). Magnetic anomalies identified from the AS map are interpreted to correspond to intrusive bodies and structurally disturbed zones that may be associated with hydrothermal mineralization.

The K/eTh ratio derived from airborne radiometric data was employed to identify hydrothermal alteration zones. Potassium is highly mobile during hydrothermal processes, whereas thorium is relatively immobile; therefore, elevated K/eTh ratios are considered diagnostic indicators of potassium enrichment associated with hydrothermal alteration (Hoover et al., 1992; Elkhateeb & Abdellatif, 2018). Areas exhibiting high K/eTh values were therefore interpreted as potential zones of hydrothermal activity and mineralization. The selected parameters were processed as raster layers within the ArcGIS 10.5 environment. Each thematic layer was reclassified into mineralization favorability classes based on their relative contribution to hydrothermal mineralization. The reclassification process considered the statistical distribution and standard deviation of each dataset to ensure consistency and proper representation of favorable zones.

Weighted Overlay

The weighted overlay technique was employed to integrate the thematic raster layers and generate a hydrothermal mineralization potential map for the Southern Benue Trough. This approach combines multiple geospatial datasets by assigning relative weights to each thematic layer according to their significance in controlling mineralization (Bonham-Carter, 1994; Feizizadeh & Blaschke, 2013). The weights assigned to the thematic layers were derived using the Analytical Hierarchy Process (AHP), which evaluates the relative importance of each parameter through pairwise comparison. Based on their influence on hydrothermal mineralization, lineament density, Analytical Signal, and K/eTh ratio were assigned suitability scores and weight percentages (Table 4). The weighted thematic layers were subsequently integrated using the weighted overlay tool in ArcGIS 10.5 to produce the final hydrothermal mineralization prospectivity map.

RESULTS AND DISCUSSION

Aeromagnetic results

First Vertical Derivative Map (FVD)

The First Vertical Derivative Map (FVDM) reveals prominent local structural anomalies trending predominantly in the NE–SW direction, with subordinate E–W, NW–SE, and WNW–ESE orientations across the Southern Benue Trough (Figure. 5). The dominant NE–SW structural trend is consistent with the regional tectonic framework of the Benue Trough and reflects the influence of Pre-Pan-African and Pan-African tectonic events on the structural evolution of the basin (Benkhelil, 1989; Anudu et al., 2014). The FVD filter effectively enhances shallow magnetic sources and emphasizes structural discontinuities such as faults, fractures, folds, and lithological contacts. These structures are interpreted as major conduits for hydrothermal fluid migration and mineralization within the study area. The enhanced structural signatures observed on the FVD map therefore provide important evidence of tectonic reactivation and structurally controlled hydrothermal activity. Short-wavelength magnetic anomalies are concentrated mainly within the north, north-east and south-eastern portions of the study area, indicating the presence of relatively shallow magnetic sources in these regions. In contrast, broader and smoother anomalies observed elsewhere are interpreted to originate from deeper magnetic sources. The concentration of shallow anomalies may be associated with intrusive bodies, faulted basement structures, and zones of tectonic deformation. The FVD map exhibits strong correspondence with the Analytical Signal (AS) map (Fig. 6), such that zones characterized by high-amplitude magnetic responses on the FVD map coincide with areas of elevated analytical signal amplitudes. These high-amplitude anomalies are interpreted to reflect magmatic intrusions, structurally deformed basement rocks, and lithological contrasts associated with granitic and metasedimentary assemblages. Similar structural patterns were also identified from the Centre for Exploration Targeting (CET) grid analysis, further confirming the structural complexity and hydrothermal significance of the study area.

Analytical Signal Map

The Analytical Signal Map (AS) delineates the edges of magnetic anomalies, structural trends, and lithological boundaries associated with variations in the magnetic properties of subsurface rocks within the Southern Benue Trough (Figure. 6). The ASM effectively enhances magnetic source boundaries independent of magnetization direction, making it particularly suitable for structural interpretation in low magnetic latitude regions such as Nigeria (Roest et al., 1992; Nabighian et al., 2005). Based on the amplitude distribution of the analytical signal, the study area was classified into three major magneto-lithologic zones: high (> 0.0166 nT/m), intermediate (0.0093 to 0.0166 nT/m), and low magnetic zones (< 0.0093 nT/m). The high magnetic zones coloured red are interpreted as areas associated with strongly magnetized basement rocks and intrusive bodies. These zones are inferred to represent magmatic intrusions emplaced within the sedimentary sequence of the Southern Benue Trough and adjoining basement terrains. The high magnetic signatures may therefore be associated with granitic intrusions, mafic bodies, tectonically deformed basement rocks, and zones of hydrothermal alteration linked to intrusive activity.

The intermediate magnetic zones are interpreted to correspond mainly to transitional lithologic units and structurally altered metasedimentary formations characterized by moderate magnetic susceptibility. These areas may reflect zones of mixed sedimentary and basement influence, including partially altered or fractured lithologies. The low magnetic zones correspond predominantly to sedimentary terrains composed mainly of shale, sandstone, limestone, clay-rich formations, and unconsolidated sediments characteristic of the Southern Benue Trough. These formations generally exhibit low magnetic susceptibility due to the absence or limited concentration of ferromagnetic minerals. The observed magnetic zonation reflects the complex tectonic and lithological framework of the Southern Benue Trough and highlights the influence of intrusive activity, basement configuration, and structural deformation on the magnetic response of the study area. Similar magnetic zonation patterns have been reported in previous aeromagnetic studies within the Benue Trough and adjacent Basement Complex terrains (Anudu et al., 2014; Oha et al., 2016).

SPI

The source parameter Imaging (SPI) module of the Oasis Montaj software was applied and it's a technique for calculating magnetic source depth from magnetic data. Depths to magnetic basementderived from the SPI technique ranged from less than 0.10 km to more than 2.7 km (Figure. 9). The entire northern, eastern, western, and southeastern portions of the map are characterized by shallow depths to basement, indicating the area in mostly underlain by the basement complex rocks and magmatic intrusions. However, parts of the central and southern zones of the Southern Benue Trough showed an increase in the depth to basement. These areas are characterized by higher sedimentary thickness suggesting that the basement rocks may have dropped to considerable depths, creating accommodation for sediment input.

The Centre for Exploration Targeting (CET) grid analysis technique was employed to extract and delineate structural features (lineaments) within the Southern Benue Trough (Figure. 7). The extracted lineaments represent major geological structures such as faults, fractures, shear zones, and lithological boundaries that are significant in controlling subsurface fluid migration and mineralization processes.

The dominant structural trends identified from the CET analysis are predominantly NE–SW, with subordinate E–W, NW–SE, and WNW–ESE orientations (Figure. 8). These structural trends are consistent with the regional tectonic framework of the Benue Trough and reflect the influence of Pre-Pan-African and Pan-African tectonic events, as well as subsequent Santonian tectonic reactivation within the basin (Benkhelil, 1989; Anudu et al., 2014).

Table 4: Parameters Employed in the Weighted Overlay Analysis for the Mineralisation Potential of the Study Area

Raster layer	Range of class	Suitability score	Suitability degree	Weight (%) assigned
Lineament density	(>0.290)	1	High	
(m/km2)	(0.12 – 0.290)	2	Moderate	33
	(<0.120	3	Low	
K/eTh (%/ppm)	(>0.0583)	1	High	
	(0.0289 – 0.583)	2	Moderate	26
	(<0.0289)	3	Low	
Analytic signal	(>0.0166)	1	High	
(nT/m)	(0.0093 - 0.0166)	2	Moderate	41
	(<0.0093)	3	Low	

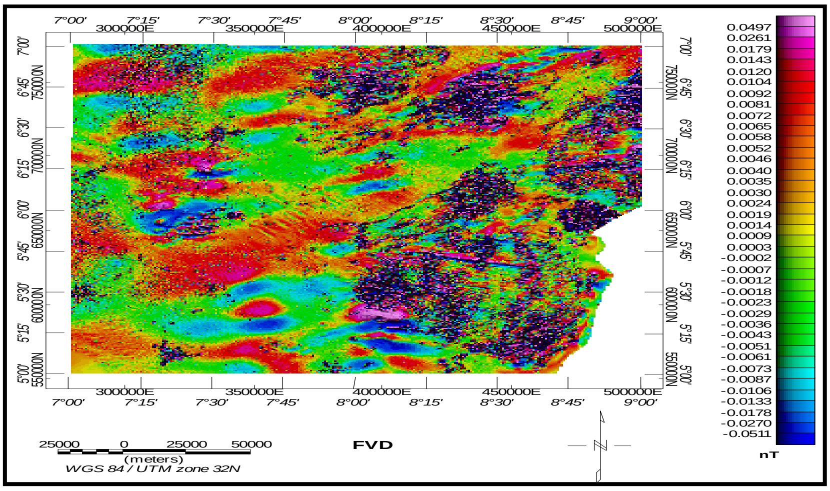

Figure 5: First Vertical Derivative map of the study area

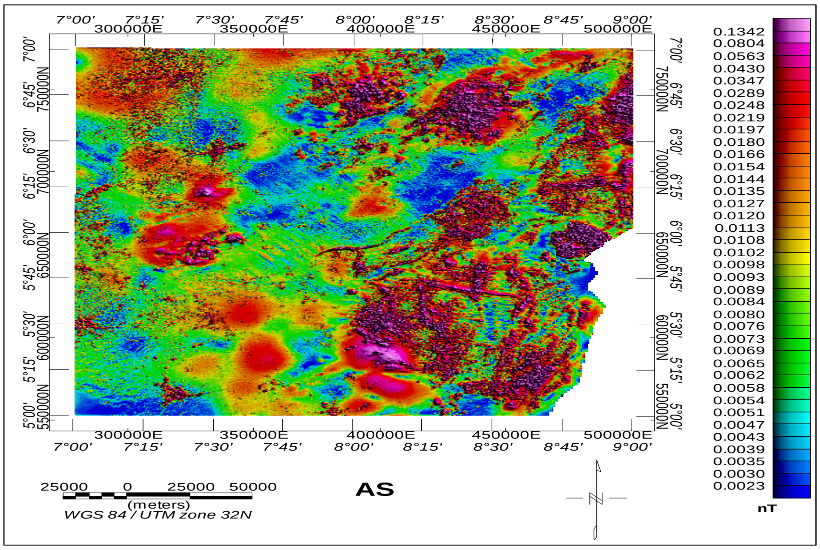

Figure 6: Analytical Signal map of the study area

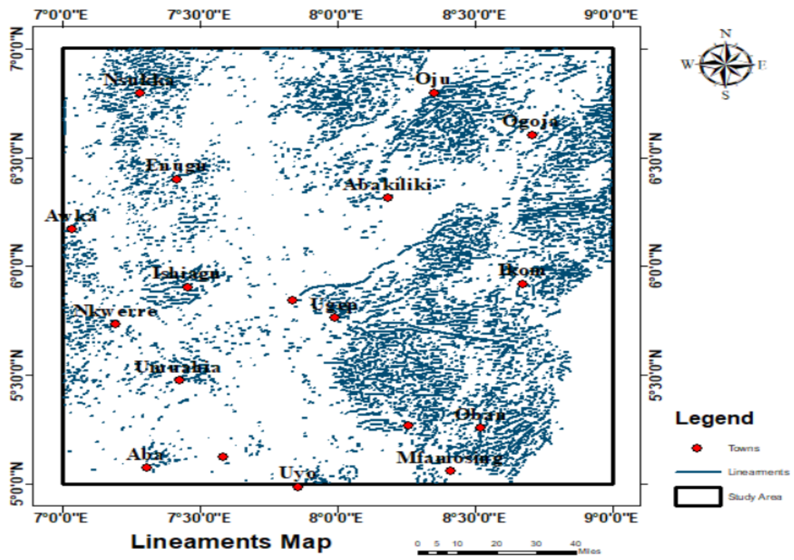

Figure 7: Lineament map of the study area

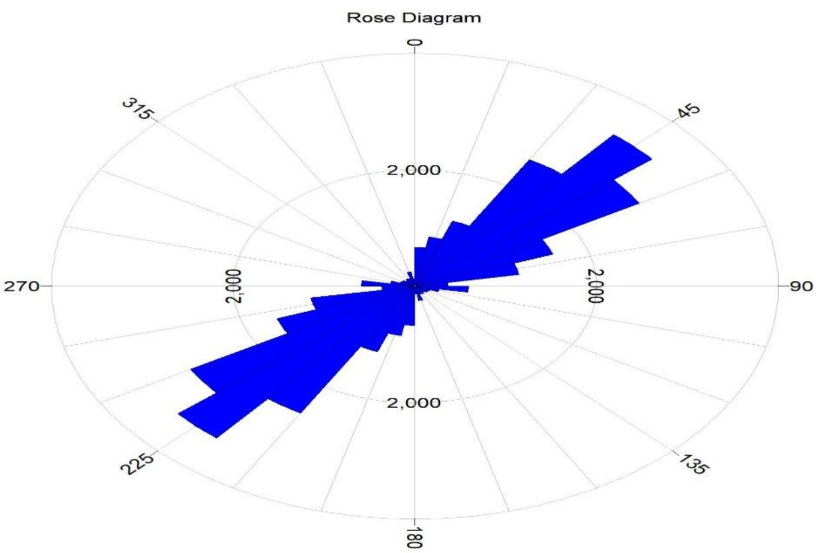

Figure 8: Rose Diagram from Lineament Map

Areas characterized by very high lineament density correspond closely with the high magnetic zones and high-frequency anomaly amplitudes observed on the Analytical Signal Map (ASM) and First Vertical Derivative Map respectively. This spatial correspondence indicates that zones of intense structural deformation are associated with shallow magnetic sources, intrusive activity, and tectonically disturbed basement rocks.

The hydrothermal mineralization potential of the study area appears to be strongly controlled by these structural features. Faults, fractures, and shear zones serve as pathways for hydrothermal fluid circulation, thereby facilitating the mobilization, concentration, and deposition of mineralizing fluids within structurally favorable zones. Consequently, regions exhibiting highlineament density are interpreted as prospective targets for hydrothermal mineralization and intrusive-related mineral systems within the Southern Benue Trough.

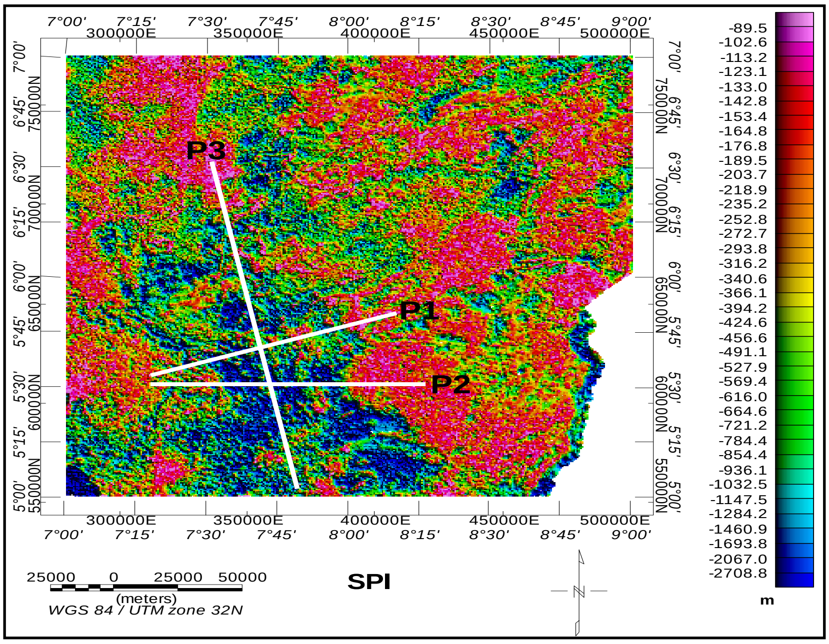

Figure 9: Source Parameter Imaging map of the study area

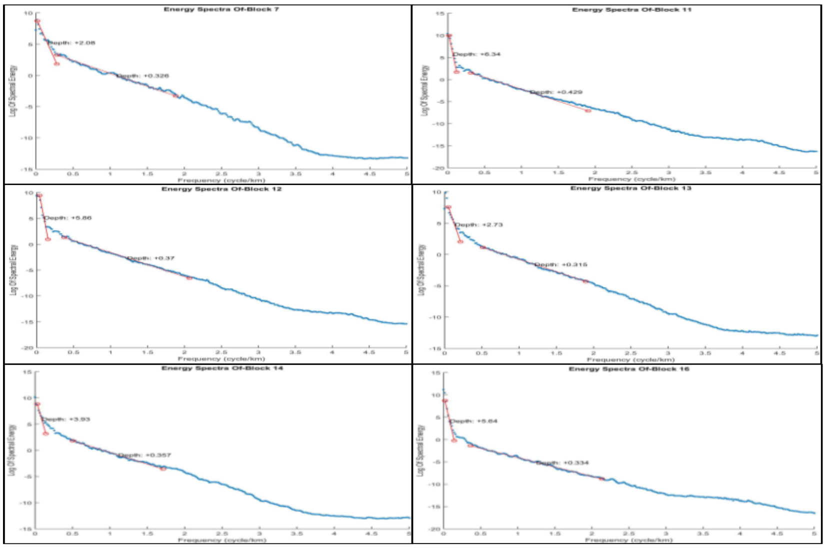
Figure 10: Depth determination graphs for shallow and deep-seated source bodies from 2D power spectrum curves of some of the analyzed blocks

Table 5: Estimated Depth to Magnetic Basement in the Study Area

Block	X	Y	Deeper Source Depths (km)	Shallower Source Depths (km)
1	306150	580750	5.18	0.244
2	334000	580950	7.99	0.223
3	361300	580550	4.98	0.292
4	389800	581400	5.78	0.503
5	417000	580950	6.27	0.319

Block	X	Y	Deeper Source Depths (km)	Shallower Source Depths (km)
6	445300	580750	7.08	0.292
7	471950	580750	2.08	0.326
8	306150	608850	4.23	0.195
9	333800	609050	6.77	0.198
10	361300	608650	5.22	0.329
in	389150	608400	6.34	0.429
12	416800	608000	5.86	0.37
13	444700	608050	2.73	0.315
14	471950	608650	3.93	0.357
15	306350	636100	4.58	0.343
16	334400	636100	5.64	0.334
17	361700	636100	7.19	0.294
18	389200	635900	9.02	0.783
19	416600	635700	3.67	0.332
20	444700	636500	3.58	0.348
21	471950	635900	3.84	0.304
22	306700	663800	4.18	0.846
23	334000	663600	5.07	0.362
24	361900	663800	5.16	0.288
25	389350	526550	5.58	0.28
26	417000	663200	5.56	0.277
27	444900	664200	2.37	0.308
28	472200	663600	3.93	0.308
29	306350	691300	3.07	0.196
30	334200	691300	4.85	0.15
31	361700	691300	4.35	0.199
32	389400	691300	4.83	0.308
33	417000	691500	5.17	0.321
34	444700	691300	3.5	0.279
35	471950	691500	1.94	0.307
36	306450	719000	6.09	0.133
37	334350	719150	4.13	0.158
38	361700	718650	4.95	0.256
39	389450	719000	5.01	0.296
40	416950	718750	5.14	0.319
41	444700	718800	5	0.377
42	472050	718900	4.5	0.336
43	306450	746400	5.69	0.216
44	334200	746350	5.84	0.155
45	362050	746550	6.02	0.311
46	389850	746400	5.14	0.317
47	417250	746750	5.3	0.345
48	444850	746400	6.75	0.39
49	472150	746650	4.35	0.34
Average			5.01	0.32

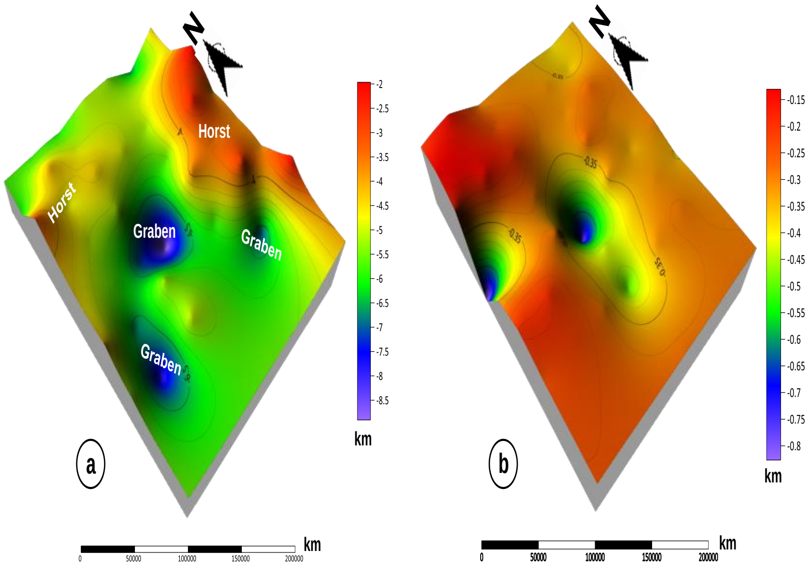

Figure. 11: 3D display of the depth to basement for (a) deeper and (b) shallow magnetic sources

Aeroradiometric Result

eU, eTh, and K% Concentration Maps

The equivalent uranium (eU) concentration map (Figure. 12) reveals spatial variations in uranium distribution across the Southern Benue Trough. High uranium concentrations ranging between 0.3002 ppm to 6.3304 ppm are mainly associated with zones of intrusive activity, structurally disturbed basement rocks, and areas characterized by hydrothermal alteration. Uranium values occur at the northern, northeastern, and parts of northwestern and southeastern portions of the region. These areas are associated with silicified sheared rocks, large quartz veins and mylonites, biotite granite, shales migmatites, sandstones, and mudstones. These high uranium anomalies are interpreted to correspond to granitic intrusions, migmatitic basement rocks, and tectonically reactivated zones within the adjoining Basement Complex and intrusive bodies emplaced withinthe sedimentary sequence (IAEA, 2003; Elkhateeb & Abdellatif, 2018; Obaje, 2009). Low uranium values mostly dominate the northwestern portion of the area, which are associated with porphyritic granite, migmatite, medium to coarse grained biotite granite, muscovite schist, fine grained biotite granite, migmatitic gneiss, mylonites interlayered with amphibolites, granite gneiss, sandstones, shales and mudstones.

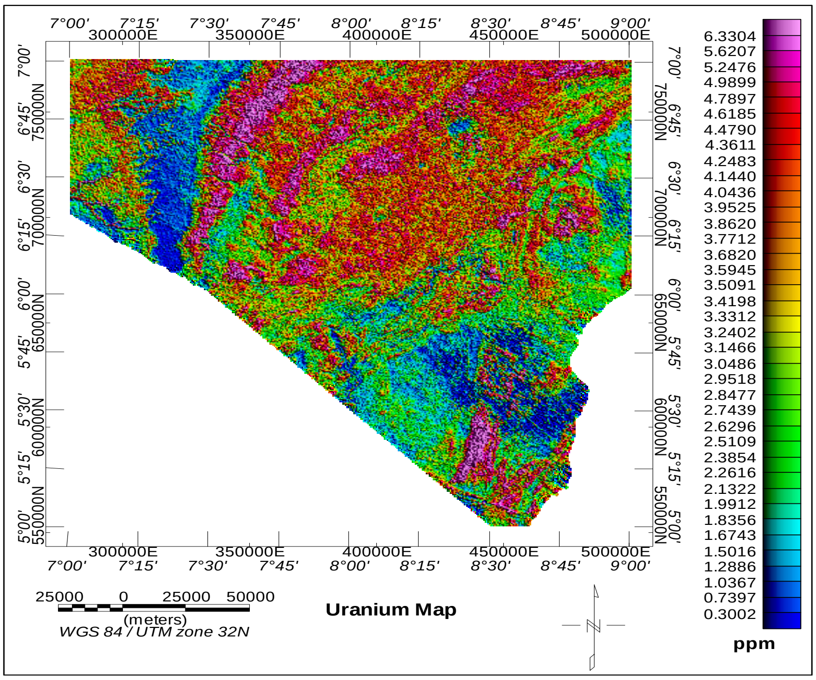

Figure. 12: Uranium Concentration Map

The concentration of thorium radioelement in the study area ranges from 3.7018 to 27.1055 ppm (Figure. 13). High thorium values are observed in the northern, northeastern, and parts ofnorthwestern and southeastern portions of the study area. The high thorium content in these zones is related to the underlying silicified sheared rocks, large quartz veins and mylonites, biotite granite, migmatites, sandstones, shales and mudstones. Low thorium levels are observed in parts of the northwestern, eastern, and southeastern zones of the region. These areas are associated with medium to coarse grained biotite granite, porphyritic granite, fine grained biotite granite, migmatite, migmatitic gneiss, muscovite schist, granite gneiss, mylonites interlayered with amphibolites, sandstones, shales and mudstones.

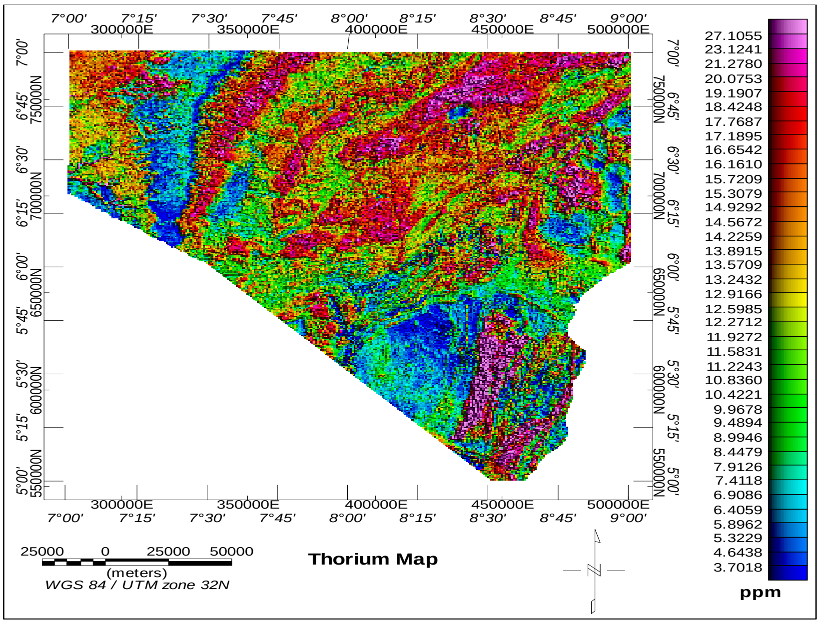

Figure 13: Thorium Concentration Map

Potassium percentage concentration values in the study area range from approximately 0.0269% to 1.8665% (Figure. 14) indicating significant spatial variation in potassium enrichment and depletion across different geological formations. These variations reflect differences in rockcomposition, degree of alteration, and structural influence on fluid migration. Areas of high potassium concentration, represented by pink, red, and purple colors, are predominantly located in the central, southeastern, and northeastern portions of the study area. These zones are interpreted as regions containing potassium-rich lithologies, such as granitic intrusions, feldspar-rich basement rocks, or hydrothermally altered formations. Potassium enrichment is commonly associated with the presence of potassium-bearing minerals such as K-feldspar, muscovite, and biotite, which are typical of felsic and intermediate rocks. The elevated potassium concentration in these areas suggests the presence of crystalline basement rocks or intrusive bodies that have undergone magmatic differentiation or hydrothermal alteration.

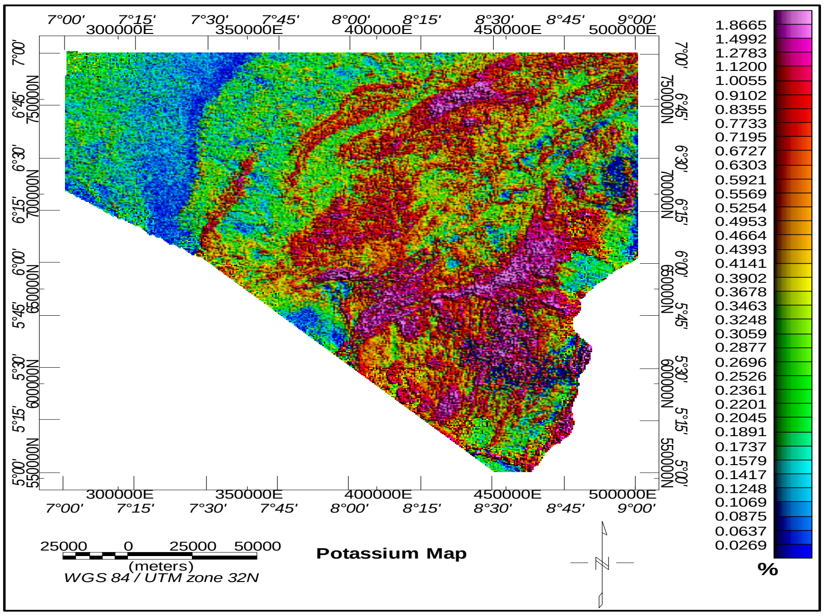

Figure 14: Potassium Concentration Map

Tenary Map

Radiometric ternary images are effective for visualizing multichannel gamma-ray spectrometry data in a single composite image (IAEA, 2003). In this study, equivalent uranium (eU), equivalent thorium (eTh), and potassium (K) were assigned blue, green, and red color channels, respectively, to evaluate lithological variation and hydrothermal alteration within the Southern Benue Trough (Figure. 15).

White-colored zones indicate high concentrations of the three radioelements and are interpreted to correspond to intrusive bodies, structurally disturbed basement rocks, and hydrothermally altered zones. In contrast, dark-colored areas represent low radioelement concentrations associated mainly with sedimentary formations such as shale, sandstone, and clay-rich units.

Red coloration indicates potassium enrichment related to potassic hydrothermal alteration, while green and blue zones represent thorium- and uranium-enriched areas, respectively (Elkhateeb & Abdellatif, 2018).

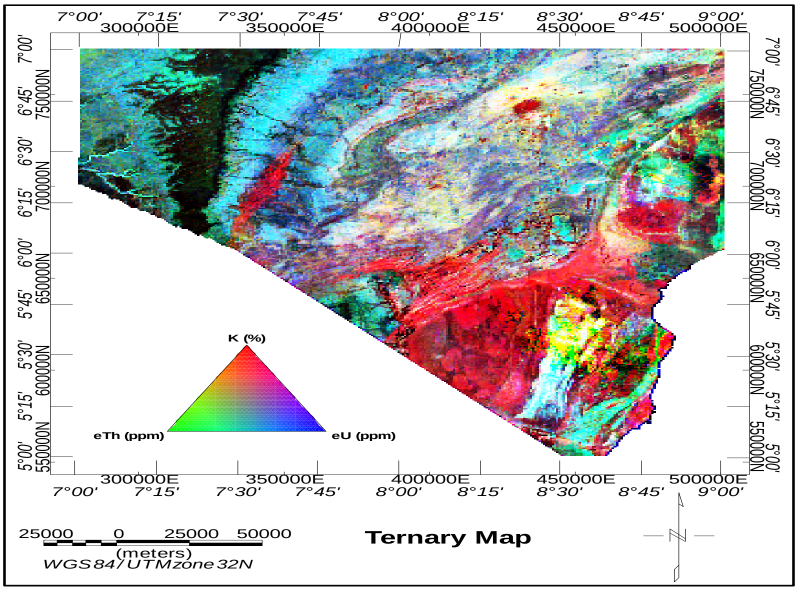

Figure 15: Ternary Map

K/Th ratio map

The K/eTh ratio map of the study area showed values ranging from 0.0024 to 0.2233 %/ppm (Figure.16), which is higher than the above stated stability range. This therefore suggests thepresence of hydrothermal mineralization occurrence in the region. High anomalous zones on the K/eTh ratio map dominate the eastern and southeastern parts of the study area. These zones have been delineated in this study to coincide with the basement rocks of the Oban Massif. The observed high K/eTh ratio anomalies are interpreted in this study to represent hydrothermally altered zones or mineralized environments in the study area. The highest K/eTh ratio values (0.2233 %/ppm) are associated with Pan-African granites, migmatites, migmatitic gneiss, porphyritic granite, and undifferentiated schist, including gneiss, fine grained flaggy quartzites, muscovite schist, and biotite granite. Low K/eTh ratio values are concentrated in the northwestern, and parts of the eastern and southeastern-most areas of the region, underlain mostly by Cretaceous sedimentary rocks.

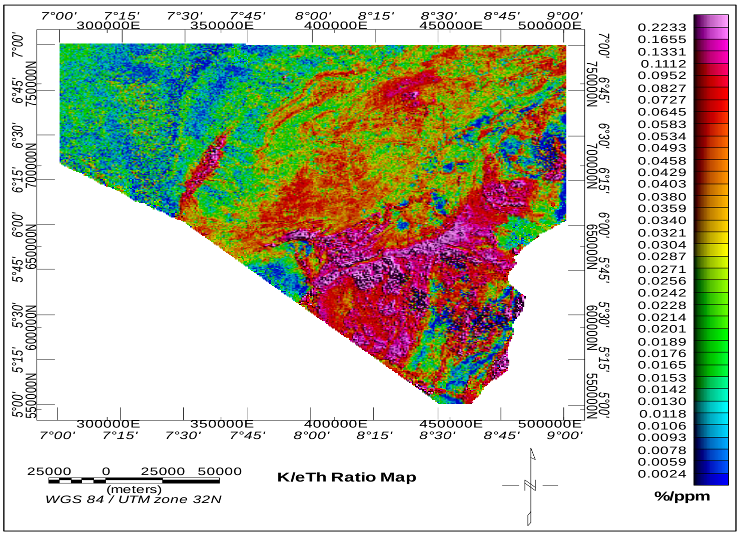

Figure 16: K/Th Ratio Map

Reclassification and spatial interoperability of results

The hydrothermal mineralization potential of the Southern Benue Trough was evaluated through the integration of selected geophysical parameters using the Analytical Hierarchy Process (AHP).

The criteria considered in the analysis include lineament density, Analytical Signal (AS), and K/eTh ratio, which were reclassified into three mineralization favorability classes: low, moderate, and high potential (Arewa James Ogah & Fahad Abubakar, 2024)

The AHP results are summarized in Table 5. The assigned weights reflect the relative importance of each parameter in controlling hydrothermal mineralization within the study area.

Table 5: AHP Results for the Mineralization Potential

Pairwise Comparison Matrix				CW1	Consistency Result
	Lineament Density	**K/Th**	**Analytical Signal**		
Lineament Density	1	1	1	0.328	C1 = 0.0278
K/Th	1	1	1/2	0.261	R1 = 0.58
Analytical Signal	1	2	1	0.411	CR = 0.0479

The Analytical Signal (AS) produced the highest cumulative weight index (CWI) of 0.411, indicating its strong influence in delineating magnetic anomalies associated with intrusive bodies and structurally controlled mineralization. Lineament density and K/eTh ratio yielded weight values of 0.328 and 0.261, respectively, reflecting the importance of structural permeability and hydrothermal alteration in mineral deposition. The consistency ratio (CR) obtained from the pairwise comparison matrix is 0.0479 (4.79%), which falls within the acceptable limit of less than 0.10 proposed by Saaty (1980). This indicates that the assigned weights and pairwise comparisons are reliable and consistent. Using the assigned weights and suitability classes, the weighted overlay tool in ArcGIS was applied to integrate the raster layers derived from the reclassified Analytical Signal (figure 17), reclassified lineament density (figure 18), and reclassified K/eTh ratio (figure 19) maps. The resulting mineral potential map (Figure. 20) delineates zones of high, moderate, and low hydrothermal mineralization potential across the Southern Benue Trough.

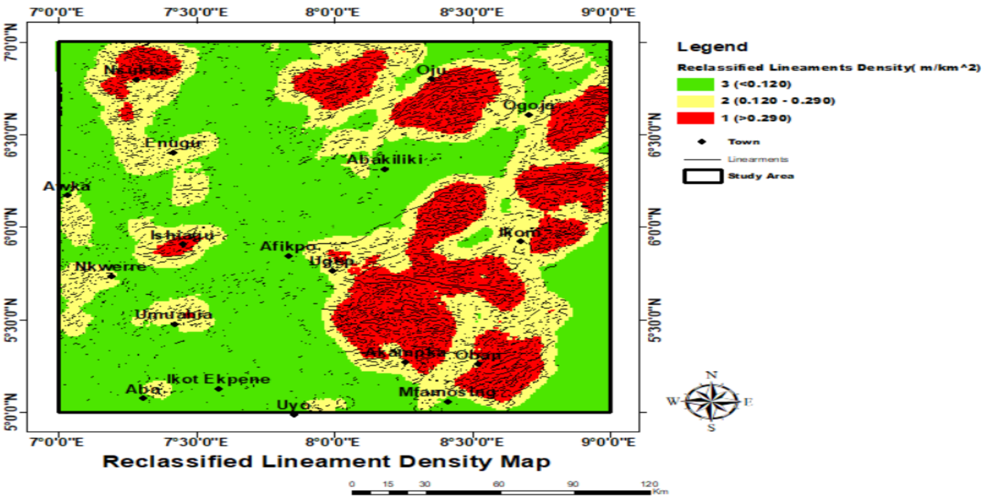

Figure 17: Reclassified Linearment Density Map of the study area

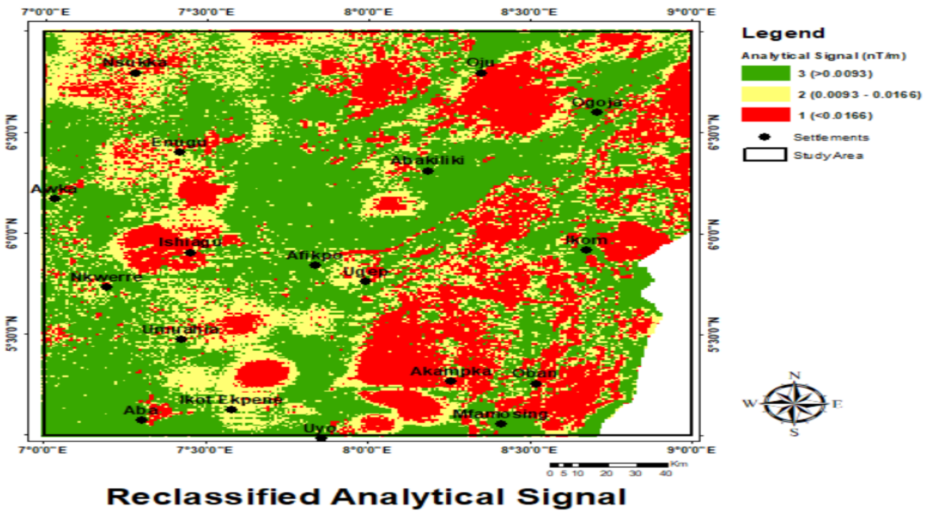

Figure 18: Reclassified Analytical Map of the study area

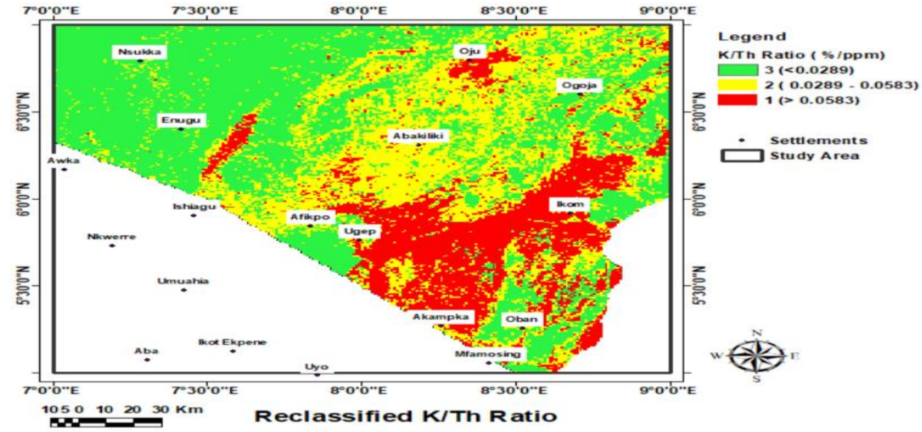

Figure 19: Reclassified K/Th Map of the study area

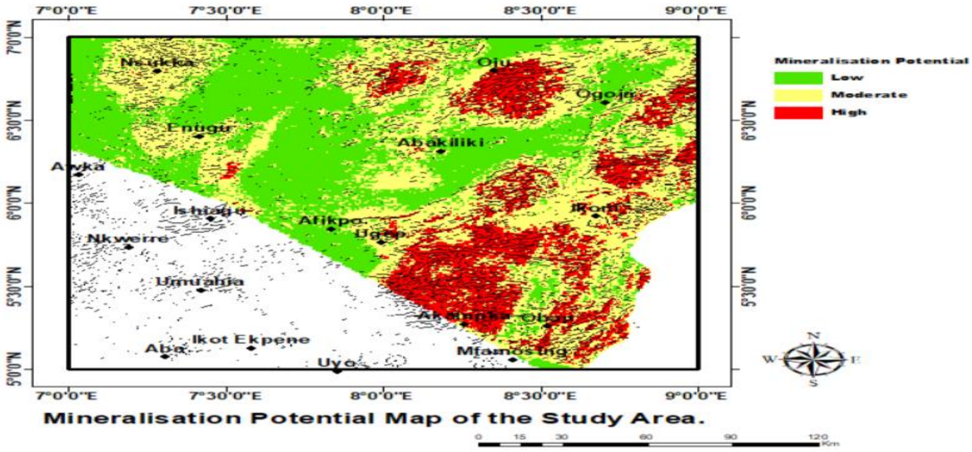

Figure 20: Mineral Potential Map of the study area

CONCLUSION

Aeromagnetic and aeroradiometric datasets were integrated using the Analytical Hierarchy Process (AHP) to evaluate the hydrothermal mineralization potential of the Southern Benue Trough. The Analytical Signal Map (ASM) delineates the edges of magnetic anomalies, structural patterns, and lithological contacts associated with variations in the magnetic properties of subsurface rocks. Based on the amplitude distribution, the study area was classified into three magneto-lithologic zones: high (> 0.0166 nT/m), intermediate (0.0093 to 0.0166 nT/m), and low magnetic zones (< 0.0093 nT/m). The high magnetic zones (HMZ) are interpreted as major magnetic source regions associated predominantly with intrusive bodies, tectonically disturbed basement rocks, and structurally deformed zones within the basin. SPI depth estimates revealed shallow magnetic source bodies ranging from <0.10 km to >2.7 km, while spectral analysis revealed deeper magnetic source depths ranging from 2.08 km to 9.02 km, with an average depth of 5.01 km. The resulting basement depth model revealed an undulating basement morphology characterized by horsts and grabens that served as depocenters for thick sedimentary accumulations. The Centre for Exploration Targeting (CET) grid analysis technique was used to extract structural lineaments within the study area. The dominant structural trends identified are E–W, NE–SW, WNW–ESE, and NW–SE, reflecting the tectonic framework of the Southern Benue Trough and adjoining Basement Complex. Zones characterized by high lineament density correspond closely with the high magnetic zones and high-frequency anomaly amplitudes observed on the ASM and First Vertical Derivative Map (FVDM), respectively. In addition, the CET porphyry analysis delineates the centers of intrusive bodies within areas of intense structural deformation and high lineament concentration. These relationships indicate that hydrothermal mineralization within the Southern Benue Trough is strongly controlled by structural features. Faults, fractures, and shear zones serve as conduits for hydrothermal fluid circulation, thereby facilitating the mobilization, concentration, and deposition of mineralizing fluids. A lineament density map was subsequently generated to further evaluate the structural control on mineralization potential across the study area. The radioelement concentration maps (eU, eTh, and K%) were also used for lithological discrimination and hydrothermal alteration mapping. The radiometric ternary image reveals highly radioactive zones and areas enriched in specific radioelements, while also delineating zones of strong potassic alteration that correspond closely with anomalies observed on the K/eTh ratio map. The K/eTh ratio map was therefore used to identify zones of hydrothermalalteration and mineralization potential. The AHP model was subsequently applied to integrate the aeromagnetic and aeroradiometric datasets. The resulting mineral prospectivity map delineates the study area into zones of high, moderate, and low hydrothermal mineralization potential. Validation using known mineral occurrence locations shows strong agreement with the model results, with 87.5% of known mineralized zones occurring within areas of high mineralization potential and 12.5% within areas of moderate potential. In addition to the known occurrences, several previously unidentified zones of prospective hydrothermal mineralization were delineated within the Southern Benue Trough.

REFERENCES

Abdelrady, M., Moneim, M. A., Alarifi, S. S., Abdelrady, A., Othman, A., Mohammed, M. A., & Mohamed, A. (2023). Geophysical investigations for the identification of subsurface features influencing mineralization zones. *Journal of King Saud University – Science, 35*(7), 102809. https://doi.org/10.1016/j.jksus.2023.102809

Abdelrady, M., Pham, L. T., Mohamed, A., Abdelrady, A., Mohammed, M. A., & Alarifi, S. S. (2024). Application of the new edge filters of aeromagnetic data to detect the subsurface structural elements controlling the mineralization in the Barramiya area, Eastern Desert of Egypt. *Journal of King Saud University – Science, 36*(1), 103539. https://doi.org/10.1016/j.jksus.2024.103539

Abdelsalam, M. G., Stern, R. J., & Copeland, P. (2020). *The Geology of North Africa*. Geological Society of London Special Publications. https://doi.org/10.1144/SP502

Agocs, W. B. (1951). Least squares residual anomaly determination. *Geophysics* 16, 686–696.

Akanbi, E. S. & Mangset, W. E. (2011). Structural trends and spectral depth analysis of the residual magnetic field of Naraguta area, North central, Nigeria. *Indian J. Sci. Technol.* 4, 1410–1415.

Akande S. O., Mücke A., & Eisenlohr B. N. (1988). Genesis of lead–zinc–barite mineralisation in the Benue Trough, Nigeria. *Mineralium Deposita*, 23, 231–239.

Akande, S. O., & Abimbola, A. F. (1987). Aspects of the genesis of lead-zinc-fluorite-barite mineralization in the Benue Trough, Nigeria. *Mineralium Deposita, 22*(2), 103–110. https://doi.org/10.1007/BF00204356.

Akande, S. O., & Mücke, A. (1993). Mineralogical, textural and paragenetic studies of the lead–zinc–fluorite–barite mineralization in the Benue Trough, Nigeria. *Mineralium Deposita, 28*(1), 22–32. https://doi.org/10.1007/BF00196330

Akingboye, A. S., Bery, A. A., Ogunyele, A. C., Gnapragasan, J., Adewumi, T., Oyeshomo, A. V., Akakuru, O. C., & Balogun, O. (2025). *Magneto–radiometric and geochemical mapping of structurally controlled hydrothermal gold mineralization in the Okpella Neoproterozoic terrain, Igarra Schist Belt, SW Nigeria*. *Scientific African, 29*, e02960. https://doi.org/10.1016/j.sciaf.2025.e02960

Allek, K., Boubaya, D., Bouguern, A., & Hamoudi, M. (2016). Spatial association analysis between hydrocarbon fields and sedimentary residual magnetic anomalies using Weights of Evidence: An example from the Triassic Province of Algeria. *Journal of Applied Geophysics, 135*, 100–110. https://doi.org/10.1016/j.jappgeo.2016.09.026

Anudu, G. K., Stephenson, R. A., & Macdonald, D. I. M. (2014). Using high-resolution aeromagnetic data to recognize and map intra-sedimentary volcanic rocks and structures in the Cretaceous Benue Trough, Nigeria. *Journal of African Earth Sciences, 99*, 625–636. https://doi.org/10.1016/j.jafrearsci.2014.06.014.

Arabameri, A., Asadi Nalivan, O., Chandra Pal, S., et al. (2021). GIS-based mineral prospectivity mapping using the analytical hierarchy process and machine learning techniques: A review. *Natural Resources Research, 30*, 2001–2028. https://doi.org/10.1007/s11053-020-09766-0

Arabameri, A., Saha, S., Roy, J., Tiefenbacher, J. P., Cerda, A., & Bui, D. T. (2021). Spatial modeling of mineral prospectivity using machine learning and multi-criteria decision-making approaches. *Geocarto International, 36*(20), 2307–2330, https://doi.org/10.1080/10106049.2020.1716751.

Benkhelil, J. (1989). The origin and evolution of the Cretaceous Benue Trough (Nigeria). *Journal of African Earth Sciences, 8*(2–4), 251–282. https://doi.org/10.1016/S0899-5362(89)80028-4.

Benkhelil, J. (1989). The origin and evolution of the Cretaceous Benue Trough (Nigeria). *Journal of African Earth Sciences (and the Middle East), 8*(2–4), 251–282. https://doi.org/10.1016/S0899-5362(89)80028-4

Blakely, R. J. (1995). *Potential Theory in Gravity and Magnetic Applications*. Cambridge University Press.

Blakely, R. J., & Simpson, R. W. (1986). Approximating edges of source bodies from magnetic or gravity anomalies. *Geophysics, 51*(7), 1494–1498. https://doi.org/10.1190/1.1442197

Bonham-Carter, G. F. (1994). *Geographic information systems for geoscientists: Modelling with GIS*. Pergamon.
British Geological Survey. (2022). *World mineral production 2016–2020*. British Geological Survey.

Burke, K., Dessauvagie, T. F. J., & Whiteman, A. J. (1971). The opening of the Gulf of Guinea and the geological history of the Benue Depression and Niger Delta. *Nature Physical Science, 233*(38), 51–55. https://doi.org/10.1038/physci233051a0.

Burke, K., Dessauvagie, T. F. J., & Whiteman, A. J. (1971). The opening of the Gulf of Guinea and the geological history of the Benue Depression and Niger Delta. *Nature Physical Science, 233*(38), 51–55.https://doi.org/10.1038/physci233051a0

Carranza, E. J. M. (2009). *Geochemical anomaly and mineral prospectivity mapping in GIS*. Elsevier. *(Book – no DOI)*

Carranza, E. J. M. (2011). Geochemical anomaly and mineral prospectivity mapping in GIS. In *Encyclopedia of GIS* (pp. 401–410). Springer. https://doi.org/10.1007/978-0-387-35973-1_594

Carranza, E. J. M. (2019). *Geochemical anomaly and mineral prospectivity mapping in GIS*. Elsevier. https://doi.org/10.1016/C2015-0-01875-7.

Dentith, M. C., Frankcombe, K. F., & Trench, A. (1994). Geophysical signatures of Western Australian mineral deposits: An overview. *AGSO Journal of Australian Geology & Geophysics, 15*(4), 125–138.

Dentith, M., & Mudge, S. T. (2014). *Geophysics for the Mineral Exploration Geoscientist*. Cambridge University Press.

Dentith, M., & Mudge, S. T. (2014). *Geophysics for the mineral exploration geoscientist*. Cambridge University Press. https://doi.org/10.1017/CBO9781139024358.

Dentith, M., & Mudge, S. T. (2014). *Geophysics for the Mineral Exploration Geoscientist*. Cambridge University Press. https://doi.org/10.1017/CBO9781139024358

Dickson, B. L., & Scott, K. M. (1997). Interpretation of aerial gamma-ray surveys—Adding the geochemical factors. *AGSO Journal of Australian Geology & Geophysics, 17*(2), 187–200.

Eldosouky, A. M., Abdelkareem, M., Elkhateeb, S. O., & Sultan, S. A. (2022). Structural analysis and basement topography of Gabal Shilman area, southeastern Desert of Egypt, using aeromagnetic data. *Journal of King Saud University – Science, 34*(3), Article 101764.

Eldosouky, A. M., Mohamed, A., Abdelrady, M., et al. (2024). Geological controls of mineralization occurrences in the Egyptian Eastern Desert: Insights from integrated aeromagnetic and remote sensing analyses. *Scientific Reports, 14*, Article 16254. https://doi.org/10.1038/s41598-024-67188-6

Elkhateeb, S. O., & Abdellatif, M. A. (2018). Delineation of hydrothermal alteration zones using airborne gamma-ray spectrometry data: A case study from Egypt. *Journal of African Earth Sciences, 147*, 34–45. https://doi.org/10.1016/j.jafrearsci.2018.06.006.

Erdi-Krausz, G., Matolín, M., Minty, B., Nicolet, J. P., Reford, W. S., & Schetselaar, E. M. (2003). *Guidelines for radioelement mapping using gamma ray spectrometry data* (IAEA-TECDOC-1363). International Atomic Energy Agency

Farrington, J. L. (1952). A preliminary description of the Nigerian lead–zinc field. *Economic Geology, 47*(6), 583–608. https://doi.org/10.2113/gsecongeo.47.6.583

Feizizadeh, B., & Blaschke, T. (2013). GIS-multicriteria decision analysis for landslide susceptibility mapping: Comparing three methods for the Urmia Lake Basin, Iran. *Natural Hazards, 65*(3), 2105–2128. https://doi.org/10.1007/s11069-012-0463-3.

Gabtni, H., & Jallouli, C. (2017). Regional-residual separation of potential field: An example from Tunisia. *Journal of Applied Geophysics, 137*, 8–24. https://doi.org/10.1016/j.jappgeo.2016.12.011

Gibert, D., & Galdeano, A. (1985). A computer program to perform transformations of gravimetric and magnetic data. *Computers & Geosciences, 11*(4), 553–588. https://doi.org/10.1016/0098-3004(85)90005-6

Holden, E.-J., Dentith, M., & Kovesi, P. (2008). Towards the automated analysis of regional aeromagnetic data to identify regions prospective for gold deposits. *Computers & Geosciences, 34*(11), 1505–1513. https://doi.org/10.1016/j.cageo.2007.08.007

Holden, E.-J., Kovesi, P., Dentith, M. C., Wedge, D., Wong, J. C., & Fu, C. S. (2010). *Detection of regions of structural complexity within aeromagnetic data using image analysis*. In *Proceedings of the 25th International Conference of Image and Vision Computing New Zealand* (pp. 1–8). IEEE. https://doi.org/10.1109/IVCNZ.2010.6148856

International Atomic Energy Agency. (2024). *Climate change and nuclear power 2024*. International Atomic Energy Agency.
International Energy Agency. (2023). *Critical minerals market review 2023*. International Energy Agency.

International Energy Agency. (2025). *Global critical minerals outlook 2025*. International Energy Agency.

Kovesi, P. (1999). Image features from phase congruency. *Videre: Journal of Computer Vision Research, 1*(3), 1–26.

Leu, L.-K. (1981). *Use of reduction-to-the-equator process for magnetic data interpretation* (Abstract). In *51st Annual International Meeting, Society of Exploration Geophysicists*. Tulsa, OK: Society of Exploration Geophysicists.

Leu, L.-K. (1982).Use of reduction-to-the-equator process for magnetic data interpretation. in *Geophysics* vol. 47 445 (Soc Exploration Geophysicists 8801 S YALE ST, TULSA, OK 74137.

Li, Y., & Oldenburg, D. W. (2001). Stable reduction to the pole at the magnetic equator. *Geophysics, 66*(2), 571–578. https://doi.org/10.1190/1.1444948

Miller, H. G., & Singh, V. (1994). Potential field tilt—A new concept for location of potential field sources. *Journal of Applied Geophysics, 32*(2–3), 213–217. https://doi.org/10.1016/0926-9851(94)90022-1

Minty, B. R. S. (1997). Fundamentals of airborne gamma-ray spectrometry. *AGSO Journal of Australian Geology & Geophysics, 17*(2), 39–50.

Nabighian, M. N. (1972). The analytic signal of two-dimensional magnetic bodies with polygonal cross-section: Its properties and use for automated anomaly interpretation. *Geophysics, 37*(3), 507–517. https://doi.org/10.1190/1.1440276

Nabighian, M. N., Grauch, V. J. S., Hansen, R. O., LaFehr, T. R., Li, Y., Peirce, J. W., Phillips, J. D., & Ruder, M. E. (2005). The historical development of the magnetic method in exploration. *Geophysics, 70*(6), 33ND–61ND. https://doi.org/10.1190/1.2133784

Nigerian Geological Survey Agency. (2022). *Geological and mineral resources map of Nigeria*. Nigerian Geological Survey Agency (NGSA).

Núñez-Demarco, P., Bonilla, A., Sánchez-Bettucci, L., & Prezzi, C. (2023). Potential-field filters for gravity and magnetic interpretation: A review. *Surveys in Geophysics, 44*(2), 603–664. https://doi.org/10.1007/s10712-022-09763-2

Nwajide, C. S. (2013). *Geology of Nigeria's sedimentary basins*. CSS Bookshops Limited.

Obaje, N. G. (2009). *Geology and mineral resources of Nigeria*. Springer. https://doi.org/10.1007/978-3-540-92685-6

Ofoegbu C. O. (1985). Interpretation of aeromagnetic anomalies over the Benue Trough, Nigeria. *Journal of African Earth Sciences*, 3(3), 307–315.

Ogunsanwo, F. O., et al. (2025). *Empirical and spatial relation between magnetic and radiometric survey over mica schist area, Ogun State, Nigeria*. FUDMA Journal of Sciences.

Oha, I. A., & Ekwueme, B. N. (2015). Structural interpretation of aeromagnetic data over the Lower Benue Trough, southeastern Nigeria. *International Journal of Geosciences*, *6*(10), 1204–1218. https://doi.org/10.4236/ijg.2015.610096

Oha, I. A., Onuoha, K. M., Nwegbu, A. N., & Abba, A. U. (2016). Interpretation of high-resolution aeromagnetic data over southern Benue Trough, southeastern Nigeria. *Journal of Earth System Science*, *125*(2), 369–385. https://doi.org/10.1007/s12040-016-0666-1

Olade, M. A. (1976). On the genesis of lead–zinc deposits in Nigeria's Benue Rift. *Economic Geology*, *71*(5), 1004–1014. https://doi.org/10.2113/gsecongeo.71.5.1004

Osinowo, O. O., Alumona, K., & Olayinka, A. I. (2020). Analyses of high-resolution aeromagnetic data for structural and porphyry mineral deposit mapping of the Nigerian Younger Granite Ring Complexes, north-central Nigeria. *Journal of African Earth Sciences*, *162*, 103705.

Oyeniyi, T. O., Salami, A. A., & Ojo, S. B. (2016). Magnetic surveying as an aid to geological mapping: A case study from Obafemi Awolowo University Campus, Ile-Ife, southwestern Nigeria. *Ife Journal of Science*, *18*(2), 331–343.

Pirajno, F. (2009). *Hydrothermal processes and mineral systems*. Springer.

Rahaman, M. A. (1988). Recent advances in the study of the Basement Complex of Nigeria. In P. O. Oluyide, W. C. Mbonu, A. E. Ogezi, I. G. Egbuniwe, A. C. Ajibade, & A. C. Umeji (Eds.), *Precambrian geology of Nigeria* (pp. 11–43). Geological Survey of Nigeria.

Rahaman, M. A. (1988). Recent advances in the study of the Basement Complex of Nigeria. In P. O. Oluyide, W. C. Mbonu, A. E. Ogezi, I. G. Egbuniwe, A. C. Ajibade, & A. C. Umeji (Eds.), *Precambrian geology of Nigeria* (pp. 11–43). Geological Survey of Nigeria.

Reyment, R. A. (1965). *Aspects of the geology of Nigeria*. Ibadan University Press.

Roest, W. R., Verhoef, J., & Pilkington, M. (1992). Magnetic interpretation using the 3-D analytic signal. *Geophysics*, *57*(1), 116–125. https://doi.org/10.1190/1.1443174

Saaty, T. L. (1980). *The analytic hierarchy process*. McGraw-Hill.

Saaty, T. L. (2008). Decision making with the analytic hierarchy process. *International Journal of Services Sciences*, *1*(1), 83–98. https://doi.org/10.1504/IJSSCI.2008.017590

Salem, A., Williams, S., Fairhead, J. D., Smith, R., & Ravat, D. (2007). Interpretation of magnetic data using tilt-angle derivatives. *Geophysics*, *72*(1), L1–L10. https://doi.org/10.1190/1.2399454

Thurston, J. B., & Smith, R. S. (1997). Automatic conversion of magnetic data to depth, dip, and susceptibility contrast using the SPI™ method. *Geophysics*, *62*(3), 807–813. https://doi.org/10.1190/1.1444190

Vacquier, V., Steenland, N. C., Henderson, R. G., & Zietz, I. (1951). *Interpretation of aeromagnetic maps* (Geological Society of America Memoir 47). Geological Society of America. https://doi.org/10.1130/MEM47-p1

Yousefi, M., & Carranza, E. J. M. (2015). Fuzzy multicriteria decision-making method for mineral prospectivity mapping. *Computers & Geosciences*, *83*, 10–25. https://doi.org/10.1016/j.cageo.2015.06.015

Yousefi, M., & Carranza, E. J. M. (2020). Prediction-area (P–A) plot and multicriteria decision-making for mineral prospectivity mapping. *Natural Resources Research*, *29*(2), 1023–1046. https://doi.org/10.1007/s11053-019-09507-5